This article is made available via the ACS COVID-19 subset for unrestricted RESEARCH re-use and analyses in any form or by any means with acknowledgement of the original source. These permissions are granted for the duration of the World Health Organization (WHO) declaration of COVID-19 as a global pandemic.

analytical chemistry

pubs.acs.org/ac Letter

Microfluidic Immunoassays for Sensitive and Simultaneous Detection of IgG/IgM/Antigen of SARS-CoV-2 within 15 min

Qiuyuan Lin,[#] Donghua Wen,[#] Jing Wu, Liling Liu, Wenjuan Wu,* Xueen Fang,* and Jilie Kong*

Cite This: https://dx.doi.org/10.1021/acs.analchem.0c01635 Read Online

ACCESS | Metrics & More | Article Recommendations | Supporting Information

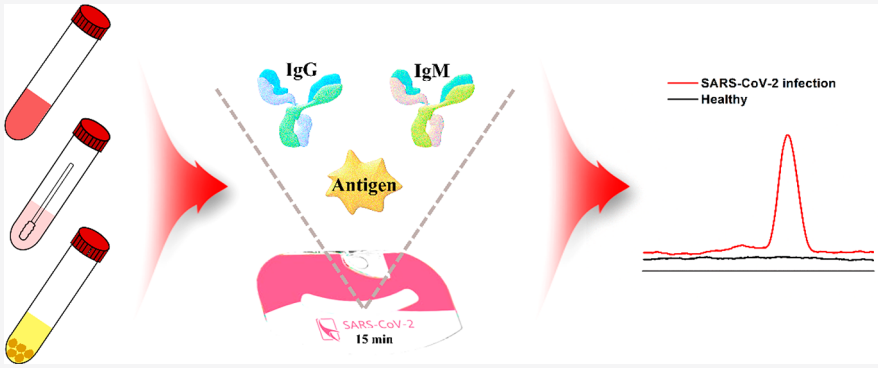

ABSTRACT: The outbreak of SARS-CoV-2 is posing serious global public health problems. Facing the emergence of this pandemic, we established a portable microfluidic immunoassay system for easy-to-use, sensitive, rapid (<15 min), multiple, and on-site detection of IgG/IgM/Antigen of SARS-CoV-2 simultaneously. This integrated method was successfully applied for detecting SARS-CoV-2 IgM and IgG antibodies in clinical human serum as well as SARS-CoV-2 antigen in pharyngeal swabs from 26 patients with COVID-19 infection and 28 uninfected people. The assay demonstrated high sensitivity and specificity, which is promising for the diagnosis and monitoring as well as control of SARS-CoV-2 worldwide.

Downloaded via 84.220.145.4 on July 13, 2020 at 12:20:11 (UTC).
See https://pubs.acs.org/sharingguidelines for options on how to legitimately share published articles.

The ongoing outbreak of severe acute respiratory syndrome coronavirus 2 (SARS-CoV-2), identified as the causative agent of the corona virus disease 2019 (COVID-19), rapidly spreads to cause a global pandemic and poses a huge challenge for global public health.[1−3] SARS-CoV-2 can spread rapidly through direct human-to-human transmission resulting in high infectivity.[4] The indefinite latency and nonspecific symptoms of SARS-CoV-2 infection makes the pandemic situation more serious.[5−8] Considering the seriously increasing number of infected cases and widening geographical spread of SARS-CoV-2, and when in absence of effective antiviral therapeutics and vaccines for COVID-19, there is an urgent need for easy-to-use, high-throughput, timely, accessible, and on-site methods for rapidly and sensitively detecting SARS-CoV-2 infection at an early stage for responses against the ongoing coronavirus outbreak and prevent and control the pandemic.[9−11]

Reverse transcription-polymerase chain reaction (RT-PCR) is the primary method for the diagnosis of SARS-CoV-2.[4,12−14] However, RT-PCR requires time-consuming and labor-intensive RNA preparation, a reverse transcription step, and professional operation, which decreases detection sensitivity and is difficult to achieve on-site detection. Computed tomography (CT) imaging is an essential tool for fast diagnosis of SARS-CoV-2.[15,16] While the specialized equipment of CT fails to meet a large scale of requirement, it may not provide the benefit for point-of-care diagnosis of COVID-19. Various enzyme-linked immunosorbent assay (ELISA)-based methods have been developed for SARS-CoV-2 diagnosis.[17] For example, the extensively utilized colloidal gold-immunochromatographic assays[18] and lateral flow immunochromatographic assays (LFAs)[19,20] offer an immunoassay method for detecting COVID-19, which show the advantages of simplicity, cost-effectiveness, fast, and point-of-care testing. Still, there are remaining limitations such as limited sensitivity and incapability of quantitative detection.

Microfluidics-based diagnostic systems have been extensively developed and applied in various fields.[21−23] Microfluidic technologies are able to integrate sample preparation, reaction, and detection steps into a miniaturized chip. Microfluidics-based platform offers many advantages: (1) it enables rapid, laboratory-quality, sensitive detection at the point of need; (2)

Received: May 22, 2020
Accepted: July 2, 2020
Published: July 2, 2020

© XXXX American Chemical Society

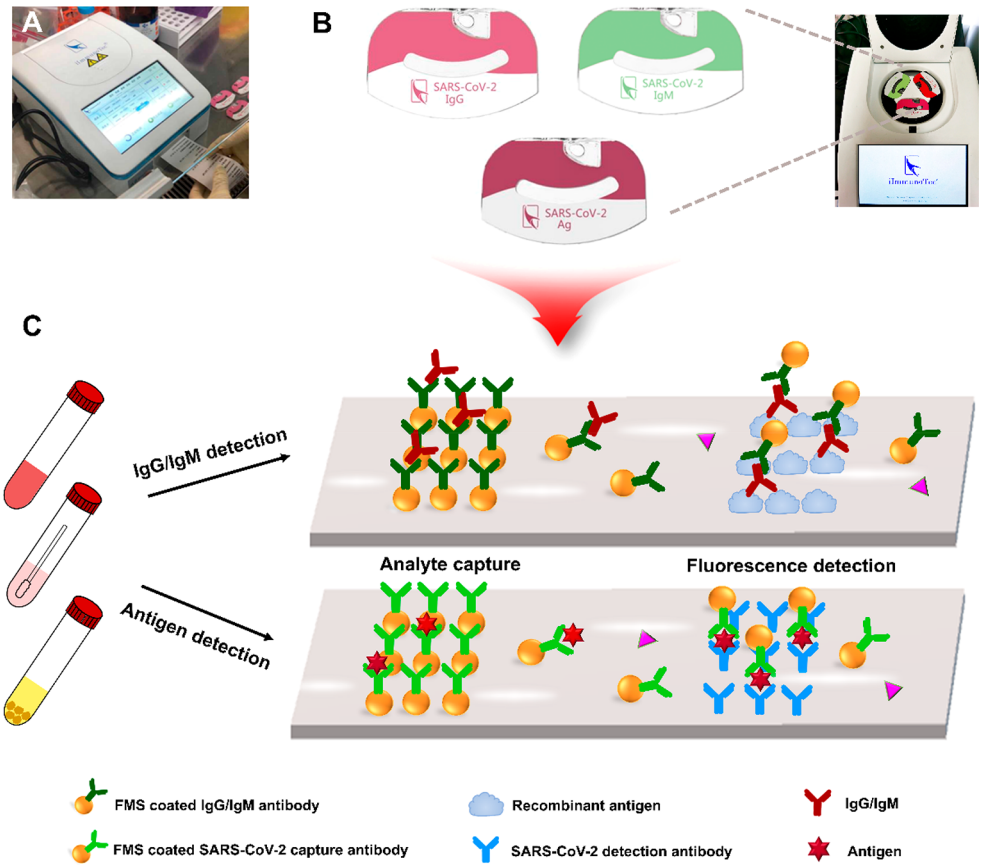

Figure 1. (A) Photograph of the portable homemade fluorescence detection equipment; (B) photograph of the immunoassay microchip ready to use; and (C) schematic illustration of the microfluidic fluorescence immunoassay for IgG/IgM/antigen detection of SARS-CoV-2.

portability, high throughput, multiplex, and automatic; (3) it significantly saves the volume of reagents and reduces the testing price.[24]

The determination of specific antibodies (such as immunoglobulin G/M, IgG/M) and antigen is an easy, fast, reliable, and accessible strategy for the diagnosis of SARS-CoV-2 as well as efficient and large-scale screening of suspected cases at point-of-care settings.[25,26] The detection of IgG and IgM in serum or whole blood has been demonstrated to be a reliable method for diagnosing COVID-19 with high specificity and sensitivity.[18,27] Additionally, detecting SARS-CoV-2 antigen protein in nasopharyngeal swab samples has exhibited outstanding advantages in clinical testing.[26]

To meet the challenge of the large epidemic, we describe the development of a point-of-care microfluidic platform integrating a homemade fluorescence detection analyzer (Figure 1A), SARS-CoV-2 diagnostic microchips (Figure 1B), and multiple immunoassays (Figure 1C) for detecting three biomarkers (IgG, IgM, and antigen). The microchip fluorescence detector (Figure 1A) measuring 28 cm × 22 cm × 14 cm and weighing 3.8 kg integrates centrifugation, fluorescence detection, and result display function, which is portable for use in the field. This proposed platform allowed analysis of three samples or biomarkers on the fluorescence detector simultaneously. The simple and low-cost microchip (length × width × height, 55 mm × 35 mm × 5.2 mm) (Figure 1B and Figure S1) was designed and fabricated by assembling top and bottom plates (made of polycarbonate) that sandwich the middle layer containing the sample analysis channel (made of double-sided adhesive tape). The microchip is composed of a sample loading chamber, a waste reservoir, and a fluorescence immunoassay fluid channel comprising a capture region and test region.

Figure 1C describes the lab-on-a-chip fluorescence immunoassay for detecting three biomarkers of SARS-CoV-2. The combination of multiple biomarker detection offers outstanding performance such as improving the sensitivity and accuracy for SARS-CoV-2 diagnosis. The preparation of the immunoassay microchip for detecting IgG, IgM, and antigen of SARS-CoV-2 was achieved by matrix nanospotting, which is listed in the Supporting Information. The cost of a ready-to-use immunoassay microchip is only about 5 yuan (0.71 dollar). When 10 μL of specimen (blood, serum, plasma, pharyngeal swabs, alveolar lavage fluid, or fecal suspension) is added into the loading chamber of the microchip followed by the addition of 70 μL of sample dilution buffer, the biomarker of SARS-CoV-2 (IgG/IgM/antigen) can specifically bind to the fluorescent microsphere (FMS) labeled capture antibody. Due to the large nanoscale of FMS, the antigen−antibody complexes are easily migrated with the flow under the capillary effect. Then the "antigen−antibody complexes" are immobilized on the fluorescence test region through a second "antigen−antibody" affinity interaction with SARS-CoV-2 antigen or detection antibody. If the specimen does not include SARS-CoV-2 biomarkers, no FMS-labeled complexes bind on the test region. After 10 min, immunoassay chips are placed in the portable fluorescence analyzer followed by 10 s centrifugation to remove the residual liquid in the channel into the waste chamber. Finally, the fluorescence detection results are read and obtained from the analyzer. The whole assay only

https://dx.doi.org/10.1021/acs.analchem.0c01635
Anal. Chem. XXXX, XXX, XXX−XXX

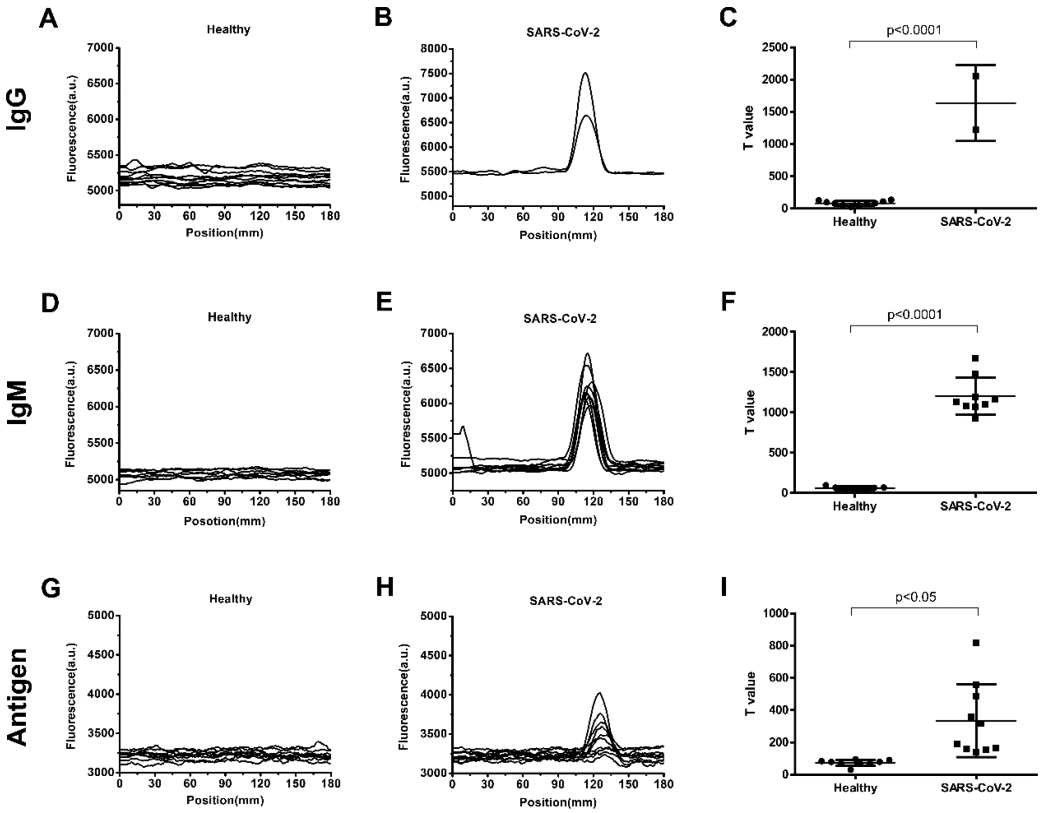

Figure 2. Fluorescence detection results of the microfluidic chip fluorescence immunoassay for SARS-CoV-2. (A and B) Fluorescence screening curve of IgG testing results from healthy people and confirmed patients; (C) comparison of *T* values from IgG testing between healthy people and confirmed patients; (D and E) Fluorescence screening curve of IgM testing results from healthy people and confirmed patients; (F) comparison of *T* values from IgM testing between confirmed patients and healthy people; (G and H) fluorescence screening curve of antigen testing results from healthy people and confirmed patients; (I) comparison of *T* values from antigen testing between healthy people and confirmed patients.

Table 1. Point-of-Care Lab-on-a-Chip Fluorescence Immunoassays Testing of Serum Specimens from COVID-19 Patients[a]

number	patient 1	patient 2	patient 3	patient 4	patient 5	healthy 1	healthy 2
days of onset	7	14	2	14	18	—	—
T value (IgG)	261.6	1197.0	338.0	723.3	2632.8	53.7	60.0
T value (IgM)	288.6	421.8	172.2	256.8	1919.1	178.5	103.2
IgG	+	++	+	++	+++	−	−
IgM	+	+	−	+	++	−	−

[a]"+" represents positive, 200−500; "++" represents medium positive, 500−1500; "+++" represents strong positive, >1500; "−" represents negative, <200).

takes less than 15 min. This robust microfluidic immunoassay system can provide a useful tool for SARS-CoV-2 diagnosis in public health laboratories as well as for timely screening potentially infected patients to monitor and prevent the epidemic owning to its capability of easy, fast, cost-effective, and point-of-care detection. Moreover, this multiple detection system contributes to enhancing the accuracy and sensitivity of the detection.

This sample-to-answer microfluidic immunoassay platform for multiple biomarkers detection was initially determined by clinical samples from confirmed COVID-19 patients and healthy samples. All clinical specimens were collected and tested in Shanghai East Hospital (affiliated East Hospital of Tongji University, Shanghai, China). Figure 2A and 2B, respectively, show the fluorescence immunoassay detection results of IgG in serum samples from 2 patients and 10 healthy people. We can observe that there is a significant difference between the infected patients and healthy people by comparing their final fluorescence value obtained from peak fluorescence intensity minus background fluorescence intensity, which was defined as the *T* value, and the *T* value could be automatically read from the analyzer (Figure 2C, $p < 0.0001$, using the Mann−Whitney no parametric test). Figure 2D−F illustrates the similar detection results of IgM in serum samples from 9 patients and 7 healthy people. The antigen testing results from nasopharyngeal swabs also exhibited an obvious distinction between 10 patients and 9 healthy people (Figure 2G−I). These results proved the feasibility of the developed method. The cutoff values for IgG, IgM, and antigen detection were determined as 200 (*T* value), 200, and 100, respectively, according to these results. It was also found that the fluorescence values of serum samples from COVID-19 patients (Figure 2B,E) were significantly higher than the detection results of pharyngeal swab samples (Figure 2H), which is probably because of the different levels of these biomarkers' concentrations between serum samples and pharyngeal swab

https://dx.doi.org/10.1021/acs.analchem.0c01635
Anal. Chem. XXXX, XXX, XXX−XXX

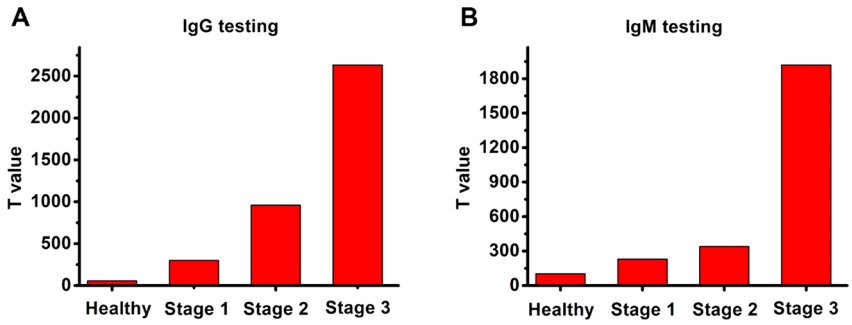

Figure 3. (A) IgG testing results of clinical samples; (B) IgM testing results of clinical samples. Healthy, uninfected sample; Stage 1, SARS-CoV-2-infected 1−7 days; Stage 2, SARS-CoV-2-infected 8−4 days; Stage 3, SARS-CoV-2-infected over 14 days.

samples. These results indicated that it was more easy and sensitive to diagnose SARS-CoV-2 infection via serum samples than pharyngeal swab samples.

The performance of the microfluidic diagnosis system was evaluated for monitoring the progression of SARS-CoV-2 infection by IgG and IgM testing. The testing results are summarized in Table 1. COVID-19 patient 1 was detected as positive in serum on the seventh day after symptom onset, and the corresponding T values for IgG/IgM were 261.6 and 288.6, respectively. COVID-19 patient 2 had positive results of IgG (T value = 1197.0) and IgM (T value = 421.8) on the 14th day. COVID-19 patient 3 was diagnosed as positive for the IgG test (T value = 338.1) and was diagnosed as negative for IgM test (T value = 172.2) on the 2nd day after onset. T values for IgG and IgM of COVID-19 patient 4 on the 14th day was 723.3 and 256.8, respectively. COVID-19 patient 5 was diagnosed as positive on the 18th day after onset with extremely high T values for IgG (T value = 2632.8) and IgM (T value = 1919.1). Two healthy samples had negative results of IgG (T value = 53.7, 60.0) and IgM (T value = 178.5, 103.2). Within the five patients, all of the IgG positives were 100% matched with clinical diagnosis results; only one false negative result of patient 2 was found for the IgM test, which is probably because the IgM level had not significantly increased on the 2nd day of infection. These results demonstrated that this immunoassay platform had a high sensitivity and specificity for the diagnosis of COVID-19, which provides a rapid approach to adequately meet the urgent need for the ongoing global outbreak management of SARS-CoV-2.

The proposed method was further evaluated by dividing the SARS-CoV-2 infection into three stages according to the patient's infection time. As shown in Figure 3A, the T value for IgG was increasing when the patients' infection time was changed from stage 1 (infected 1−7 days) to stage 3 (infected over 14 days). Such a growth trend was also observed when detecting IgM in serum from COVID-19 patients (Figure 3B). These findings further proved that the microchip immunoassay could not only accurately identify between SARS-CoV-2-infected and uninfected cases but also roughly discriminate the severity of the patient's infection development with high sensitivity and reliability. The proposed microfluidic immunoassay exhibits the comparable superiority with the traditional colloidal gold-immunochromatographic assay method for SARS-CoV-2 detection,[18] such as easy-to-use, low cost, and point-of-care detection. Moreover, our method offers the ability of sensitive, multiple, and quantitative detection based on fluorescence intensity (T value), which shows promising applications for COVID-19 diagnosis. Our method has been approved by the Center for Medical Device Evaluation (CMDE) in China and obtained European CE certification.

In conclusion, this study successfully developed a multiple detection tool for diagnosis of SARS-CoV-2, which integrated diagnostic microchips, a homemade portable fluorescence detector, and a microfluidic immunoassay approach. The multiple-testing platform was demonstrated to be easy-to-use, rapid, portable, and highly sensitive for point-of-care detection of SARS-CoV-2 within 15 min. The novel integrated diagnostic tool holds great promise for applications in SARS-CoV-2 pandemic monitoring and control. Meanwhile, this sample-to-answer system is expected to be readily applicable for quantitative and sensitive detection of biomarkers of many diseases.

■ ASSOCIATED CONTENT

Supporting Information

The Supporting Information is available free of charge at https://pubs.acs.org/doi/10.1021/acs.analchem.0c01635.

Figure S1, scheme of microchip for fluorescence immunoassay; experimental section including materials, conjugation of fluorescent microspheres with capture antibodies, preparation of the immunoassay microchip, and immunoassays on a microchip (PDF)

■ AUTHOR INFORMATION

Corresponding Authors

Xueen Fang − *Shanghai Suxin Biotechnology Co. Ltd., Shanghai 201318, P. R. China; NingBo iGeneTec Technology Co. Ltd., Ningbo 315000, P. R. China; Department of Chemistry and Institutes of Biomedical Sciences, Fudan University, Shanghai 200433, P. R. China;* orcid.org/0000-0002-3266-7868; Email: fxech@fudan.edu.cn

Jilie Kong − *Shanghai Suxin Biotechnology Co. Ltd., Shanghai 201318, P. R. China; NingBo iGeneTec Technology Co. Ltd., Ningbo 315000, P. R. China; Department of Chemistry and Institutes of Biomedical Sciences, Fudan University, Shanghai 200433, P. R. China*; Email: jlkong@fudan.edu.cn

Wenjuan Wu − *Department of Laboratory Medicine, Shanghai East Hospital, Tongji University School of Medicine, Shanghai 200123, P. R. China*; Email: wwj1210@126.com

Authors

Qiuyuan Lin − *Shanghai Suxin Biotechnology Co. Ltd., Shanghai 201318, P. R. China; NingBo iGeneTec Technology Co. Ltd., Ningbo 315000, P. R. China; Department of Chemistry and Institutes of Biomedical Sciences, Fudan University, Shanghai 200433, P. R. China*

https://dx.doi.org/10.1021/acs.analchem.0c01635
Anal. Chem. XXXX, XXX, XXX−XXX

Donghua Wen − *Department of Laboratory Medicine, Shanghai East Hospital, Tongji University School of Medicine, Shanghai 200123, P. R. China*

Jing Wu − *Shanghai Suxin Biotechnology Co. Ltd., Shanghai 201318, P. R. China; NingBo iGeneTec Technology Co. Ltd., Ningbo 315000, P. R. China*

Liling Liu − *Shanghai Suxin Biotechnology Co. Ltd., Shanghai 201318, P. R. China; NingBo iGeneTec Technology Co. Ltd., Ningbo 315000, P. R. China*

Complete contact information is available at: https://pubs.acs.org/10.1021/acs.analchem.0c01635

Author Contributions

[#]Q.L. and D.W. are first co-authors. All authors have given approval to the final version of the manuscript.

Notes

The authors declare no competing financial interest.

■ ACKNOWLEDGMENTS

We thank the National Key R & D Program of China (Grant 2017YFA0205100), the National Natural Science Foundation of China (Grant 21974028), and the Natural Science Foundation of Shanghai (Grants 19441903900, 12ZR1401700, and 17JC1400100) for financial support.

■ REFERENCES

(1) Wang, C.; Horby, P. W.; Hayden, F. G.; Gao, G. F. *Lancet* **2020**, *395*, 470−473.

(2) Hui, D. S.; Azhar, E. I.; Madani, T. A.; Ntoumi, F.; Kock, R.; Dar, O.; Ippolito, G.; Mchugh, T. D.; Memish, Z. A.; Drosten, C.; Zumla, A.; Petersen, E. *Int. J. Infect. Dis.* **2020**, *91*, 264−266.

(3) Nasir, J. A.; Speicher, D. J.; Kozak, R. A.; Poinar, H. N.; Miller, M. S.; McArthur, A. G. *Preprints* **2020**, 2020020385.

(4) Chu, D. K. W.; Pan, Y.; Cheng, S. M. S.; Hui, K. P. Y.; Krishnan, P.; Liu, Y.; Ng, D. Y. M.; Wan, C. K. C.; Yang, P.; Wang, Q.; Peiris, M.; Poon, L. L. M. *Clin. Chem.* **2020**, *66*, 549−555.

(5) Backer, J. A.; Klinkenberg, D.; Wallinga, J. *Eurosurveillance* **2020**, *25* (5), 2000062.

(6) Wang, D.; Hu, B.; Hu, C.; Zhu, F.; Liu, X.; Zhang, J.; Wang, B.; Xiang, H.; Cheng, Z.; Xiong, Y.; Zhao, Y.; Li, Y.; Wang, X.; Peng, Z. *JAMA* **2020**, *323* (11), 1061−1069.

(7) Huang, C.; Wang, Y.; Li, X.; Ren, L.; Zhao, J.; Hu, Y.; Zhang, L.; Fan, G.; Xu, J.; Gu, X.; Cheng, Z.; Yu, T.; Xia, J.; Wei, Y.; Wu, W.; Xie, X.; Yin, W.; Li, H.; Liu, M.; Xiao, Y.; et al. *Lancet* **2020**, *395*, 497−506.

(8) Chen, N.; Zhou, M.; Dong, X.; Qu, J.; Gong, F.; Han, Y.; Qiu, Y.; Wang, J.; Liu, Y.; Wei, Y.; Xia, J. a.; Yu, T.; Zhang, X.; Zhang, L. *Lancet* **2020**, *395*, 507−513.

(9) Chen, Z. M.; Fu, J. F.; Shu, Q.; Chen, Y. H.; Hua, C. Z.; Li, F. B.; Lin, R.; Tang, L. F.; Wang, T. L.; Wang, W.; Wang, Y. S.; Xu, W. Z.; Yang, Z. H.; Ye, S.; Yuan, T. M.; Zhang, C. M.; Zhang, Y. Y. *World J. Pediatr.* **2020**, *16*, 240.

(10) Shen, K.; Yang, Y.; Wang, T.; Zhao, D.; Jiang, Y.; Jin, R.; Zheng, Y.; Xu, B.; Xie, Z.; Lin, L.; Shang, Y.; Lu, X.; Shu, S.; Bai, Y.; Deng, J.; Lu, M.; Ye, L.; Wang, X.; Wang, Y.; Gao, L. *World J. Pediatr.* **2020**, *16*, 223.

(11) Pang, J.; Wang, M. X.; Ang, I. Y. H.; Tan, S. H. X.; Lewis, R. F.; Chen, J. I-P.; Gutierrez, R. A; Gwee, S. X. W.; Chua, P. E. Y.; Yang, Q.; Ng, X. Y.; Yap, R. K.S.; Tan, H. Y.; Teo, Y. Y.; Tan, C. C.; Cook, A. R.; Yap, J. C.-H.; Hsu, L. Y. *J. Clin. Med.* **2020**, *9*, 623.

(12) Konrad, R.; Eberle, U.; Dangel, A.; Treis, B.; Berger, A.; Bengs, K.; Fingerle, V.; Liebl, B.; Ackermann, N.; Sing, A. *Euro Surveill* **2020**, *25* (9), 2000173.

(13) Pfefferle, S.; Reucher, S.; Norz, D.; Lutgehetmann, M. *Euro Surveill* **2020**, *25* (9), 2000152.

(14) Corman, V. M.; Landt, O.; Kaiser, M.; Molenkamp, R.; Meijer, A.; Chu, D. K. W.; Bleicker, T.; Brunink, S.; Schneider, J.; Schmidt, M. L.; Mulders, D.; Haagmans, B. L.; van der Veer, B.; van den Brink, S.; Wijsman, L.; Goderski, G.; Romette, J. L.; Ellis, J.; Zambon, M.; Peiris, M.; et al. *Euro Surveill* **2020**, *25* (3), 2000045.

(15) Song, Y.; Zheng, S.; Li, L.; Zhang, X.; Zhang, X.; Huang, Z.; Chen, J.; Zhao, H.; Jie, Y.; Wang, R.; Chong, Y.; Shen, J.; Zha, Y.; Yang, Y. *medRxiv* **2020**, DOI: 10.1101/2020.02.23.20026930.

(16) Chung, M.; Bernheim, A.; Mei, X.; Zhang, N.; Huang, M.; Zeng, X.; Cui, J.; Xu, W.; Yang, Y.; Fayad, Z. A.; Jacobi, A.; Li, K.; Li, S.; Shan, H. *Radiology* **2020**, *295*, 202−207.

(17) Traugott, M.; Aberle, S. W.; Aberle, J. H.; Griebler, H.; Karolyi, M.; Pawelka, E.; Puchhammer-Stöckl, E.; Zoufaly, A.; Weseslindtner, L. *J. Infect. Dis.* **2020**, *222*, 362.

(18) Li, Z.; Yi, Y.; Luo, X.; Xiong, N.; Liu, Y.; Li, S.; Sun, R.; Wang, Y.; Hu, B.; Chen, W.; Zhang, Y.; Wang, J.; Huang, B.; Lin, Y.; Yang, J.; Cai, W.; Wang, X.; Cheng, J.; Chen, Z.; Sun, K. *J. Med. Virol.* **2020**, DOI: 10.1002/jmv.25727.

(19) Van Elslande, J.; Houben, E.; Depypere, M.; Brackenier, A.; Desmet, S.; Andre, E.; Van Ranst, M.; Lagrou, K.; Vermeersch, P. *Clin. Microbiol. Infect.* **2020**, DOI: 10.1016/j.cmi.2020.05.023.

(20) Ong, D. S. Y.; de Man, S. J.; Lindeboom, F. A.; Koeleman, J. G. M. *Clin. Microbiol. Infect.* **2020**, DOI: 10.1016/j.cmi.2020.05.028.

(21) Han, K. N.; Li, C. A.; Seong, G. H. *Annu. Rev. Anal. Chem.* **2013**, *6*, 119−141.

(22) Chin, C. D.; Laksanasopin, T.; Cheung, Y. K.; Steinmiller, D.; Linder, V.; Parsa, H.; Wang, J.; Moore, H.; Rouse, R.; Umviligihozo, G.; Karita, E.; Mwambarangwe, L.; Braunstein, S. L.; van de Wijgert, J.; Sahabo, R.; Justman, J. E.; El-Sadr, W.; Sia, S. K. *Nat. Med.* **2011**, *17*, 1015−1019.

(23) Ng, A. H. C.; Fobel, R.; Fobel, C.; Lamanna, J.; Rackus, D. G.; Summers, A.; Dixon, C.; Dryden, M. D. M.; Lam, C.; Ho, M.; Mufti, N. S.; Lee, V.; Asri, M. A. M.; Sykes, E. A.; Chamberlain, M. D.; Joseph, R.; Ope, M.; Scobie, H. M.; Knipes, A.; Rota, P. A.; Marano, N.; Chege, P. M.; Njuguna, M.; Nzunza, R.; Kisangau, N.; Kiogora, J.; Karuingi, M.; Burton, J. W.; Borus, P.; Lam, E.; Wheeler, A. R. *Sci. Transl. Med.* **2018**, *10* (438), No. eaar6076.

(24) Ye, X.; Li, L.; Li, J.; Wu, X.; Fang, X.; Kong, J. *ACS Sensors* **2019**, *4*, 3066−3071.

(25) Li, B.; Feng, F.; Yang, G.; Liu, A.; Yang, N.; Jiang, Q.; Zhang, H.; Wang, T.; Li, P.; Mao, Y.; Li, B. *SSRN J.* **2020**, DOI: 10.2139/ssrn.3543609.

(26) Seo, G.; Lee, G.; Kim, M. J.; Baek, S. H.; Choi, M.; Ku, K. B.; Lee, C. S.; Jun, S.; Park, D.; Kim, H. G.; Kim, S. J.; Lee, J. O.; Kim, B. T.; Park, E. C.; Kim, S. I. *ACS Nano* **2020**, *14*, 5135−5142.

(27) Cai, X.-f.; Chen, J.; Hu, J.-l.; Long, Q.-x.; Deng, H.-j.; Liu, P.; Fan, K.; Liao, P.; Liu, B.-z.; Wu, G.-c.; Chen, Y.-k.; Li, Z.-j.; Wang, K.; Zhang, X.-l.; Tian, W.-g.; Xiang, J.-l.; Du, H.-x.; Wang, J.; Hu, Y.; Tang, N.; Lin, Y.; Ren, J.-h.; Huang, L.-y.; Wei, J.; Gan, C.-y.; Chen, Y.-m.; Gao, Q.-z.; Chen, A-m.; He, C.-l.; Wang, D.-X.; Hu, P.; Zhou, F.-C.; Huang, A.-l.; Wang, D.-q. *J. Infect. Dis.* **2020**, *222*, 189.

Supporting information

Microfluidic Immunoassays for Sensitive and Simultaneous Detection of IgG/IgM/Antigen of SARS-CoV-2 within 15 min

Qiuyuan Lin[a,c], Donghua Wen[b,#], Jing Wu[a], Liling Liu[a], Wenjuan Wu[b,*], Xueen Fang,[a,c,*] and Jilie Kong [a,c,*]

[a]Shanghai Suxin Biotechnology Co. Ltd, and IgeneTec Diagnostic products Co. Ltd. Shanghai 201318, P. R. China

[b]Department of Laboratory Medicine, Shanghai East Hospital, Tongji University School of Medicine, Shanghai 200123, P. R. China

[c]Department of Chemistry and Institutes of Biomedical Sciences, Fudan University, Shanghai 200433, P. R. China

Corresponding Authors:
Xueen Fang, fxech@fudan.edu.cn;
Jilie Kong, jlkong@fudan.edu.cn;
Wenjuan Wu, wwj1210@126.com

Table of contents:

1. Figure S1
2. Experimental

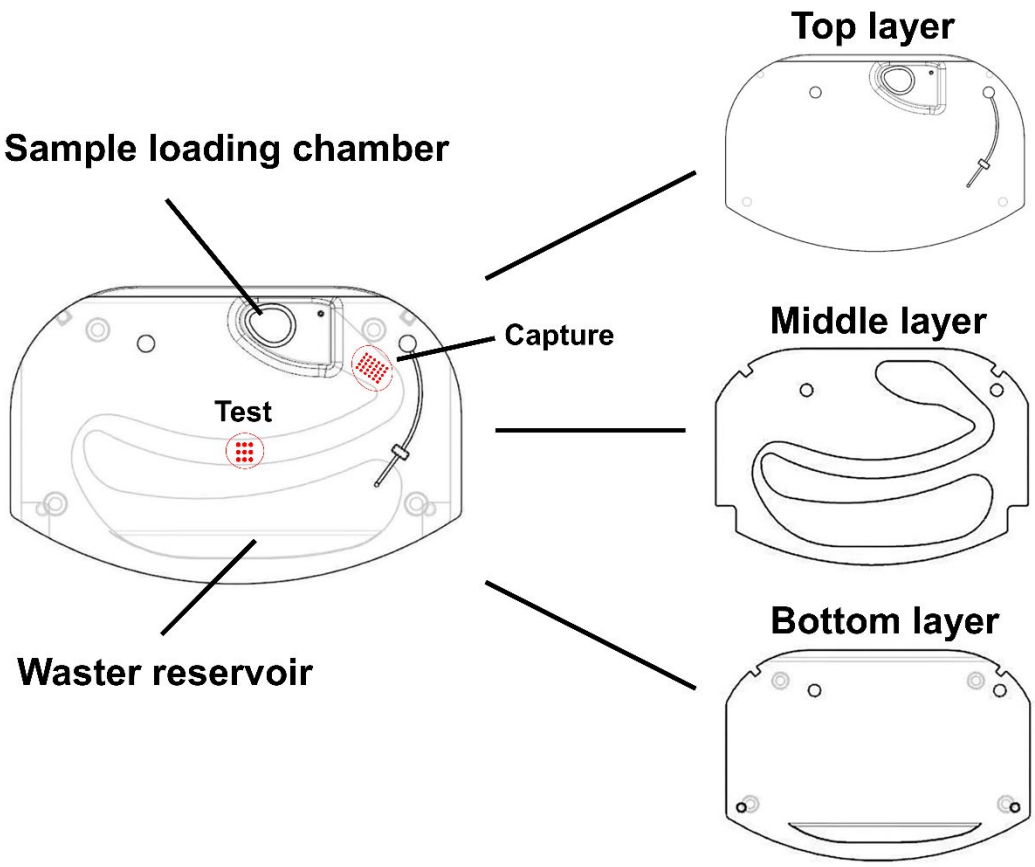

Figure S1. Scheme of microchip for fluorescence immunoassay. (Capture: FMS labeled mouse anti-human IgG/IgM antibody or SARS-CoV-2 capture antibody (rabbit anti-human polyclonal antibody) was patterned in order to capture analyte; Test: SARS-CoV-2 antigen or SARS-CoV-2 detection antibody (mouse anti-human monoclonal antibody) was patterned in order to capture FMS labeled complexes for fluorescence detection.)

Experimental

Materials

Mouse anti-human IgG/IgM antibody, SARS-CoV-2 antigen (recombinant antigen), SARS-CoV-2 capture antibody (rabbit anti-human polyclonal antibody) and SARS-CoV-2 detection antibody (mouse anti-human monoclonal antibody) and sample buffer (0.1M PBS, pH 7.4, 0.1% TX-100) were from Shanghai Suchuang Diagnostic Products Co., Ltd. (Shanghai, China). Fluoro-max dyed carboxylate-modified microparticles (fluorescent microspheres, 200 nm,) and sulfo-NHS were obtained from Thermo Fisher Scientific (China) Co., Ltd. (Shanghai, China). 1-(3-dimethylaminopropyl)-3-ethylcarbodiimide hydrochloride (EDC) and bovine serum albumin (BSA) were purchased from Sigma Aldrich Trading Co., Ltd. (Shanghai, China). 2-(N-morpholino) ethanesulfonic acid sodium salt (MES sodium salt, 50 g) was obtained from Sangon Biotech (Shanghai) Co., Ltd. (Shanghai, China). Microchips were manufactured by Shanghai Suchuang Diagnostic Products Co., Ltd. (Shanghai, China).

A portable microchip instrument (Shanghai Suchuang Diagnostic Products Co., Ltd, consists of three parts: a microchip base bracket with centrifugation function, a laser-induced fluorescence detector, and a display. The microchip instrument enables to analyze three immunoassay microchips each time.

Clinical samples such as serum and pharyngeal swabs were collected and tested in Shanghai East Hospital (affiliated East Hospital of Tongji University, Shanghai, China). The written informed consent had been obtained since the start of the project. All

experiments on clinical samples were performed in compliance with the Medical Research Ethics Committee, Shanghai Pediatric Hospital. All of clinical samples were detected directly in this assay and each extra sample was stored at -20 °C for further study.

Conjugation of fluorescent microspheres with capture antibodies.

The conjugation of fluorescent microspheres (FMS) with capture antibody against IgG/IgM/Antigen was achieved according to the manufacturer's instructions with minor modification. FMS were coated with each type of capture antibody through amide bond under the activation of EDC and NHS.

Preparation of immunoassay microchip.

Detection antibody of each marker (IgG/IgM/Antigen) and antigen against SARS-CoV-2 were patterned on the surface of bottom substrate layer of a microchip by matrix nano-spotting strategy (Ad3220 Aspirate/Dispense Platform (BIODOT, USA)). 0.5 μL of 0.5 mg/mL SARS-CoV-2 antigen (recombinant antigen) (for IgG/IgM detection) or SARS-CoV-2 detection antibody (for antigen detection) was spotted onto the test region in a matrix of 3×3 spots (each spot ~ 50 nL); 3 μL of FMS coated mouse anti-human IgG/IgM capture antibody or SARS-CoV-2 capture antibody (rabbit anti-human polyclonal antibody) (1.08 mg/mL) was spotted onto capture region in a matrix of 5×6 spots (each spot ~ 100 nL). The patterned bottom layers were then dried at 37 °C for 4 h. Finally, the immunoassay microchips were assembled by the double-sided adhesive layer and stored at 2-30 °C for use.

Immunoassays on microchip

The fluorescence immunoassay detection of IgG/IgM/Antigen in the developed microchips was performed as follows. 10 μL of sample was directly added to sample loading chamber and followed by 70 μL of sample buffer**,** then the microchip targeting one of the analytes (IgG/IgM/Antigen) and incubated for 10 min. Three immunoassay chips were placed in the portable immunoassay microchip instrument in a single run and centrifuged for seconds to remove the residual liquid in the channels following fluorescence detection for 1 min. The fluorescence intensity of test (T value) can be automatically obtained from the instrument for sample analysis.